Science Advances
AAAS

Supplementary Materials for

Transformation of arginine into zero-dimensional nanomaterial endows the material with antibacterial and osteoinductive activity

Jiaying Li *et al.*

Corresponding author: Bin Li, binli@suda.edu.cn; Fengxuan Han, fxhan@suda.edu.cn;
Xiaodong Xing, xingxiaodong07@njust.edu.cn

Sci. Adv. **9**, eadf8645 (2023)
DOI: 10.1126/sciadv.adf8645

This PDF file includes:

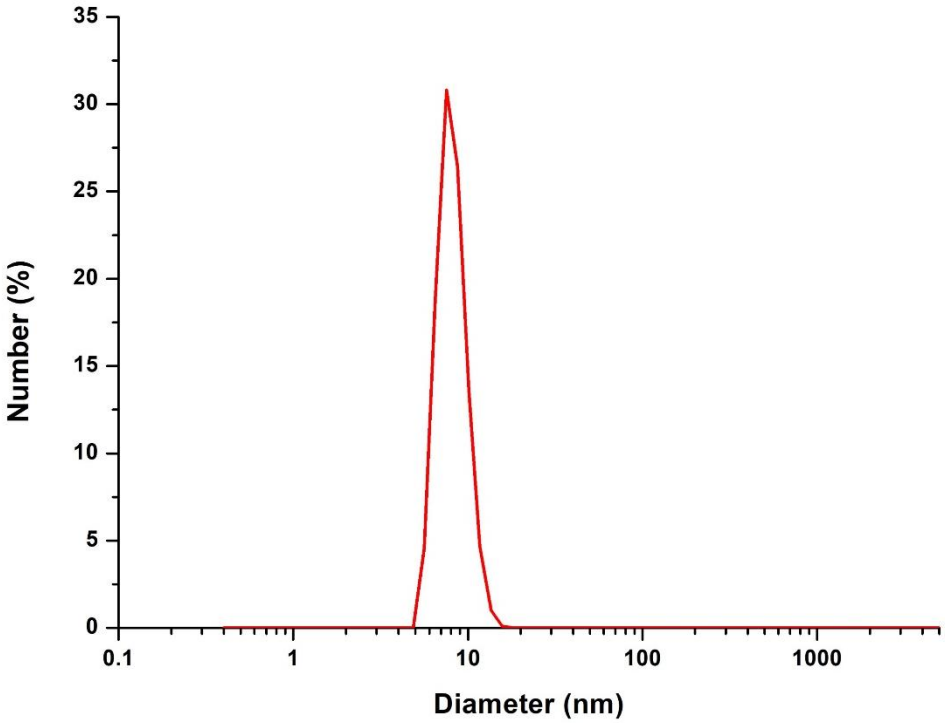

Fig. S1. Diameter distribution of Arg-CDs.

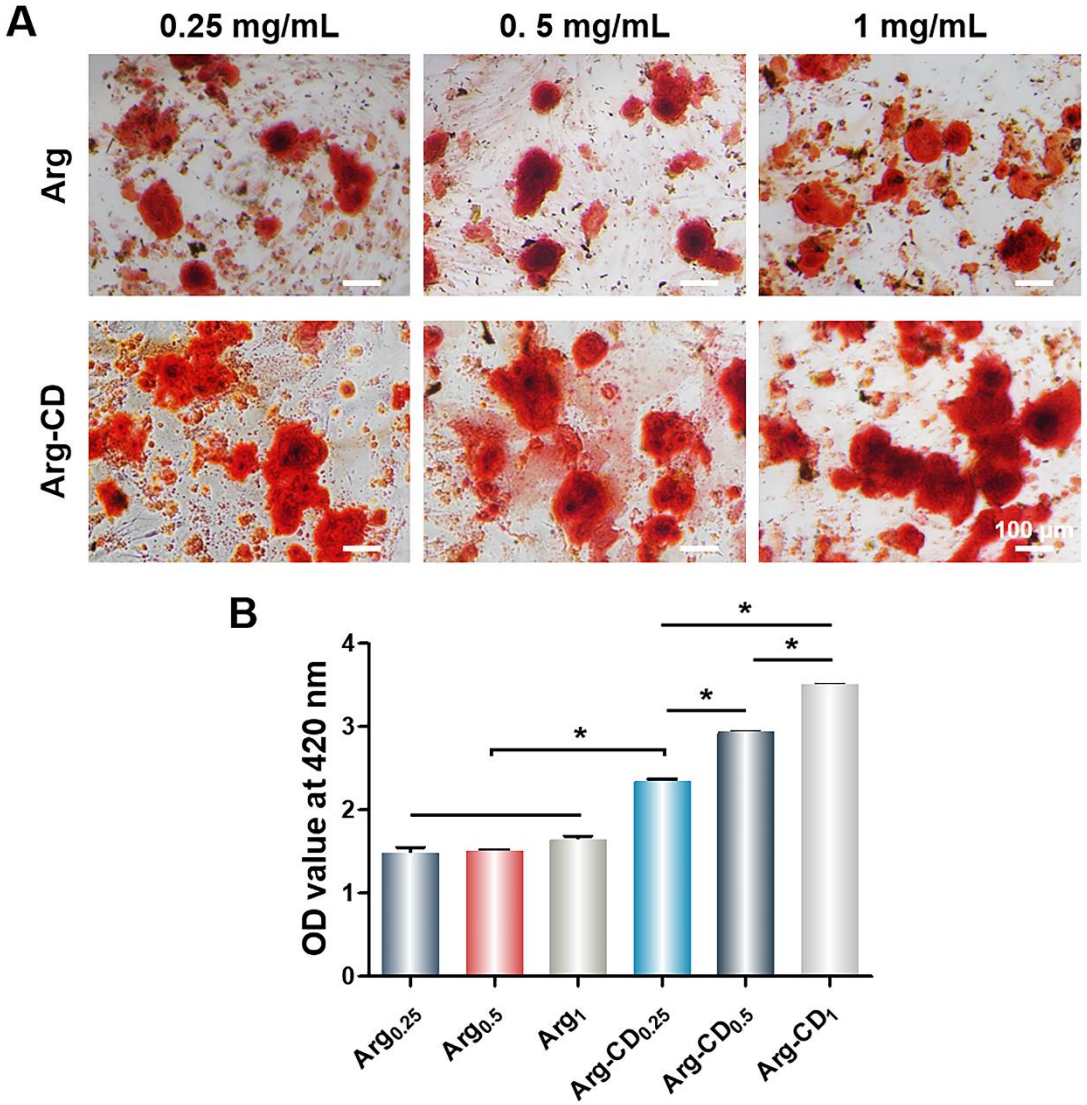

Fig. S2. Alizarin red staining (**A**) and quantitative characterization (**B**) of calcium deposition in BMSCs after treatment by Arg and Arg-CDs.

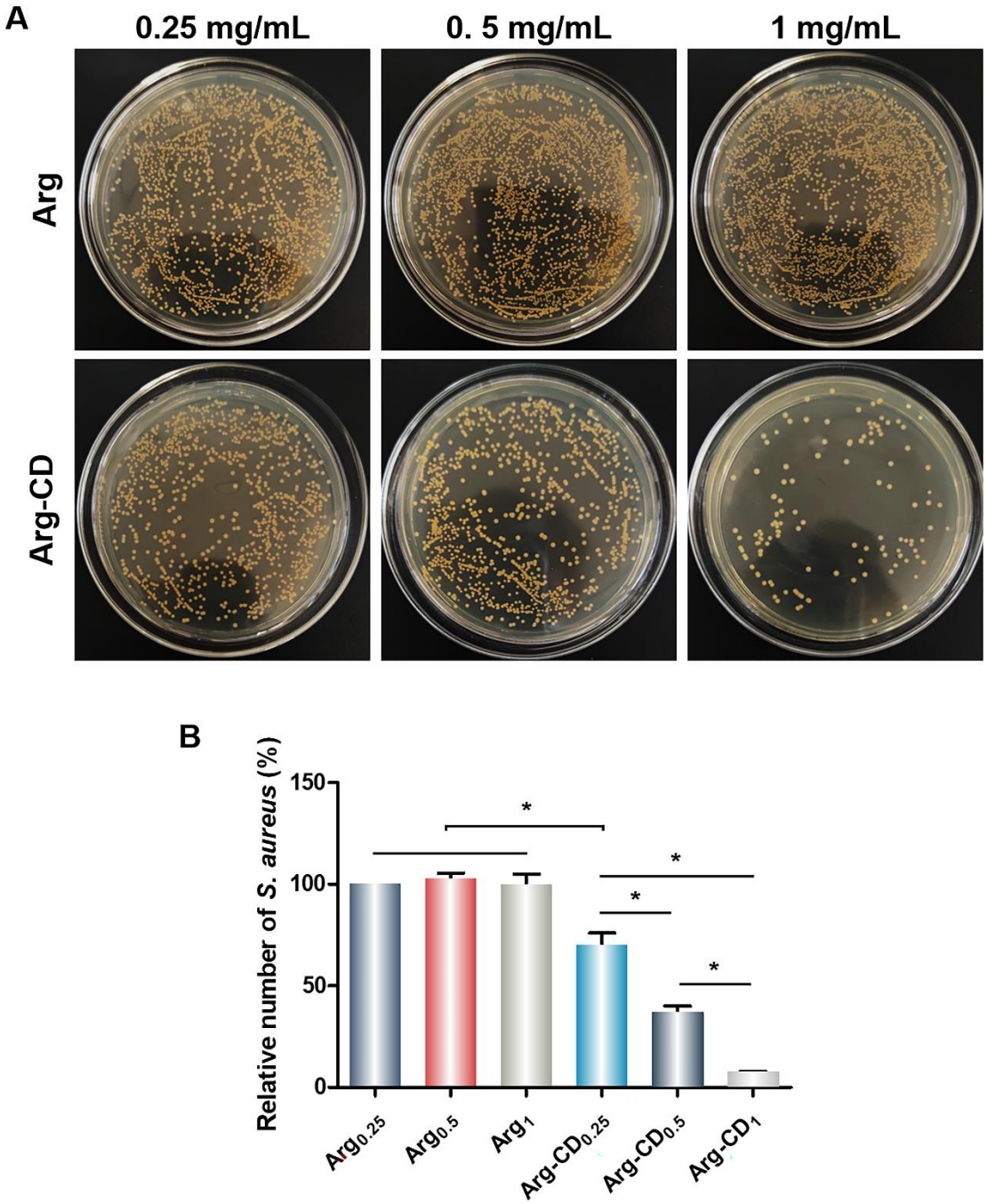

Fig. S3. Colonies of *S. aureus* counted after treatments with Arg and Arg-CDs.

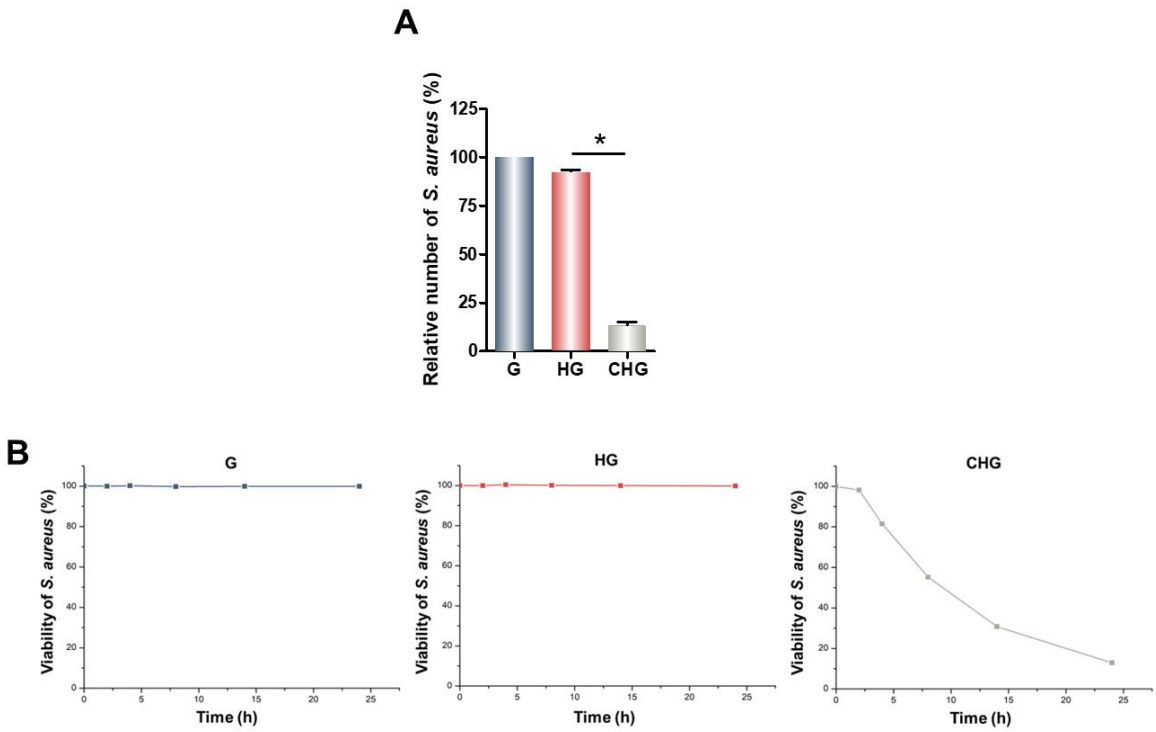

Fig. S4. Quantification (**A**) and viability curve (**B**) of *S. aureus* treated by composite hydrogels. (*$p < 0.05$)

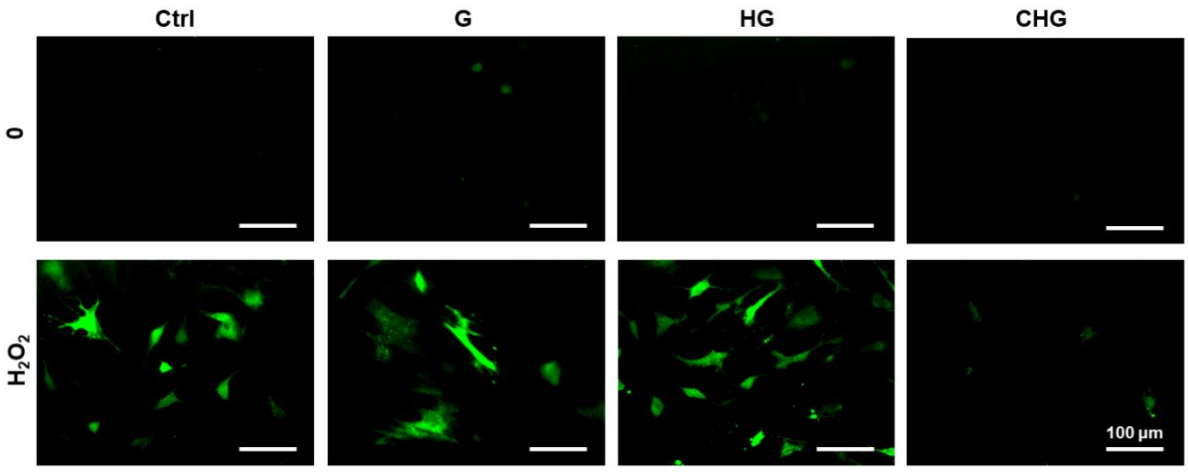

Fig. S5. DCFH-DA staining for detection of ROS level in BMSCs seeded on composite hydrogels.

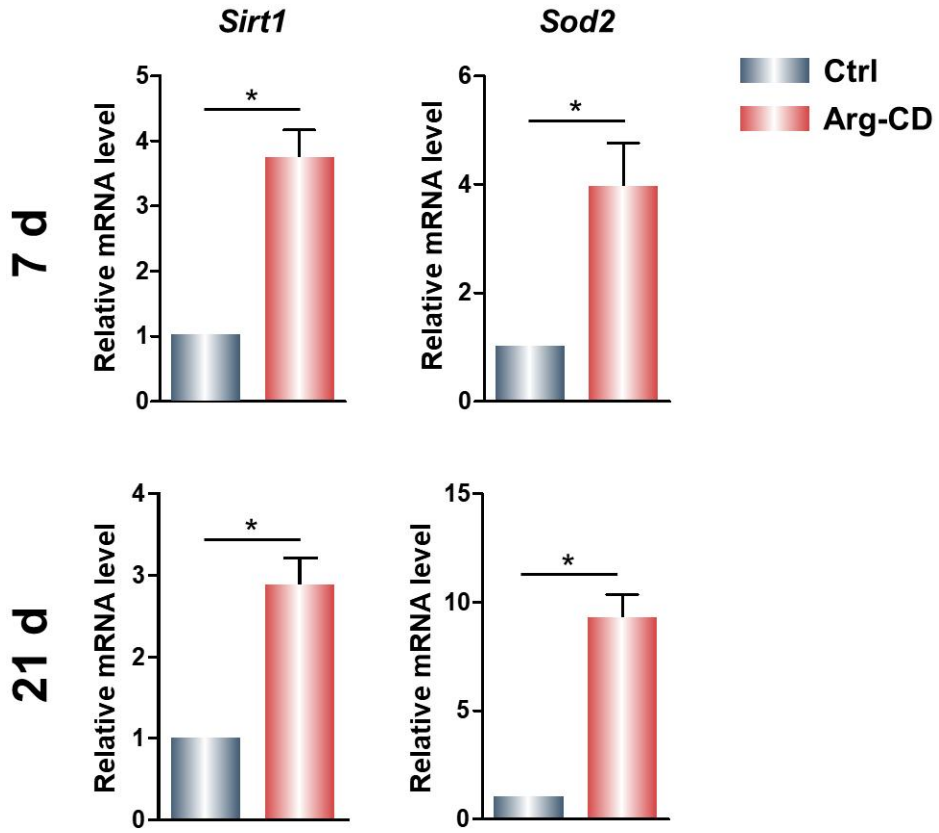

Fig. S6. Expression of antioxidant genes of BMSCs cultured with Arg-CDs. (*$p < 0.05$)

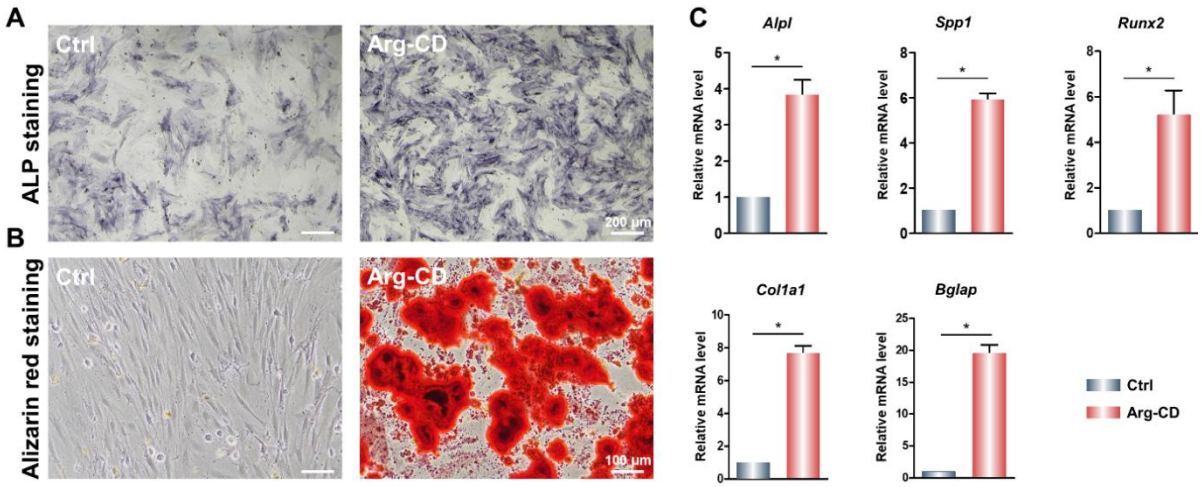

Fig. S7. *In vitro* osteogenesis of BMSCs cultured with Arg-CDs. (**A**) ALP staining of BMSCs cultured with Arg-CDs. (**B**) Alizarin red staining of BMSCs cultured with Arg-CDs. (**C**) Expression of osteogenesis-related genes of BMSCs cultured with Arg-CDs. (*$p < 0.05$)

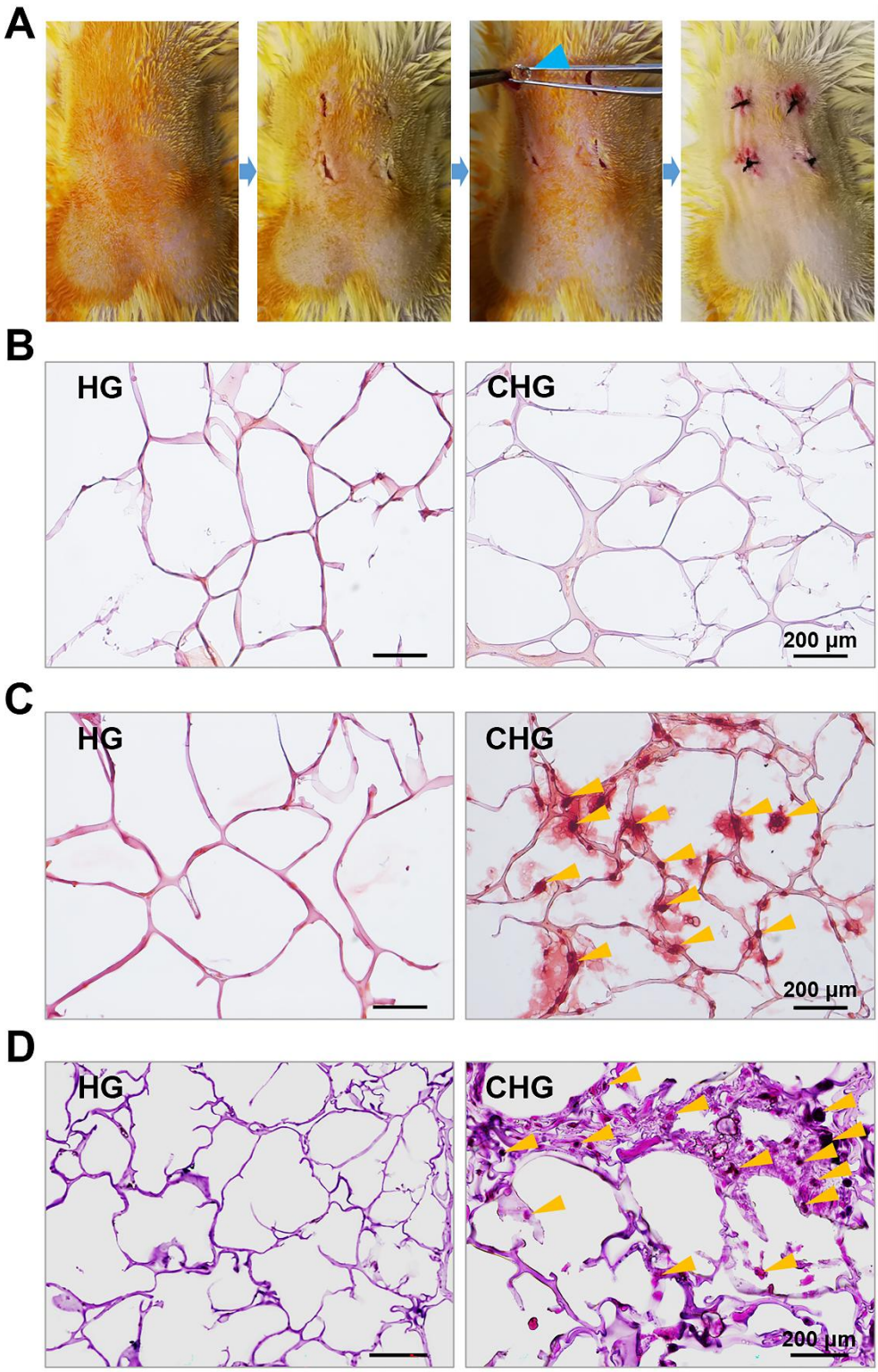

Fig. S8. The process of implanting composite hydrogels subcutaneously (**A**) and the alizarin red staining (**B**: preimplantation; **C**: postimplantation) and H&E staining (**D**) at 4 weeks after implantation.

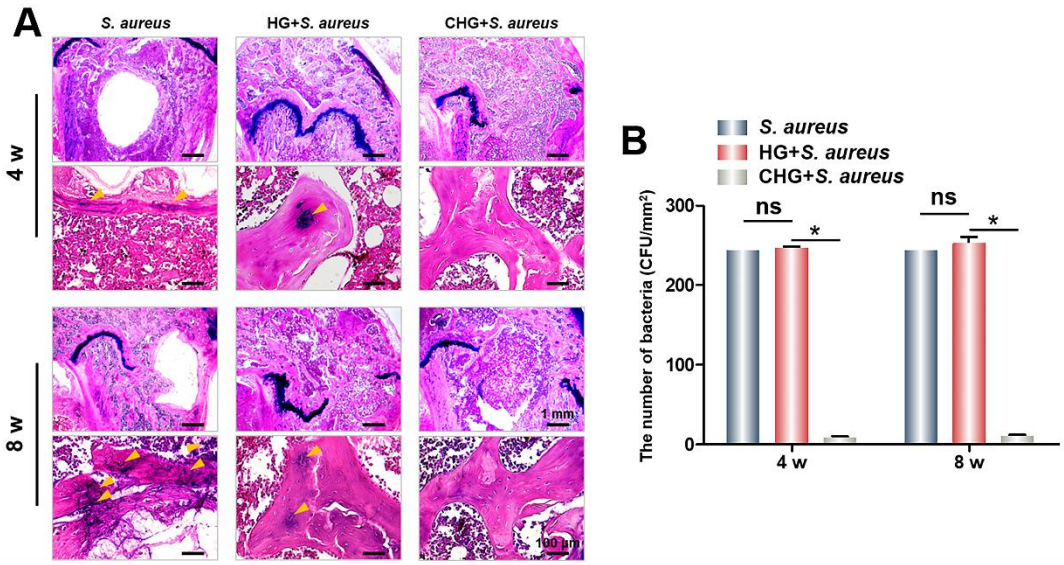

Fig. S9. Giemsa staining (**A**) and quantitative analysis (**B**) of bacteria at femoral critical-sized defects in rats. (*$p < 0.05$)

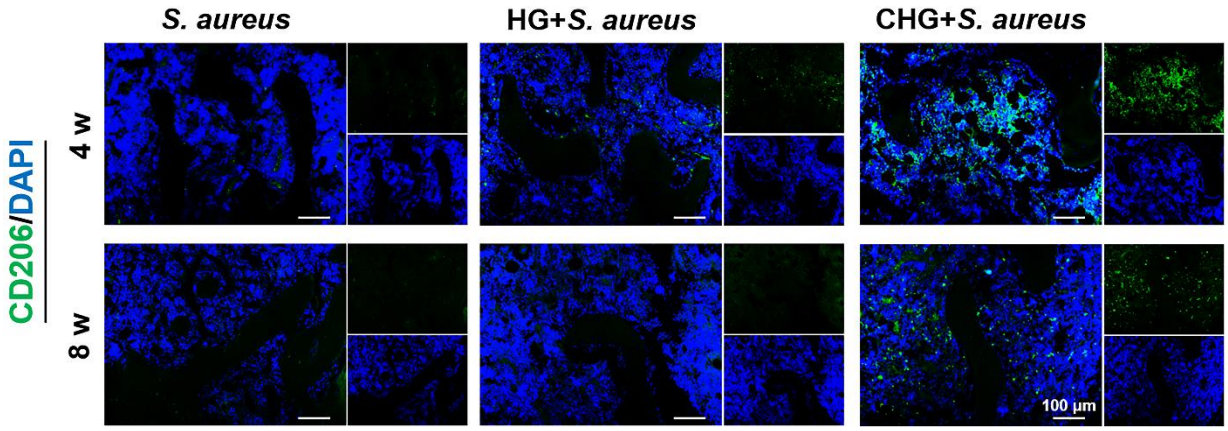

Fig. S10. Immunofluorescence of macrophages infiltration in the infection site. In each figure, the enlarged one in the left shows the merged image, and the thumbnails in the right show individual images from each channel.

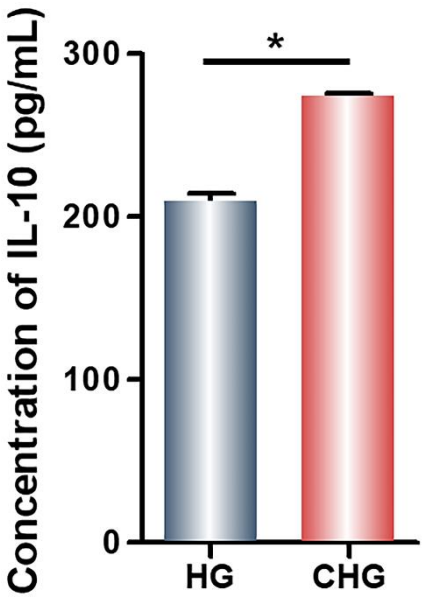

Fig. S11. Detection of IL-10 released from BMMs.

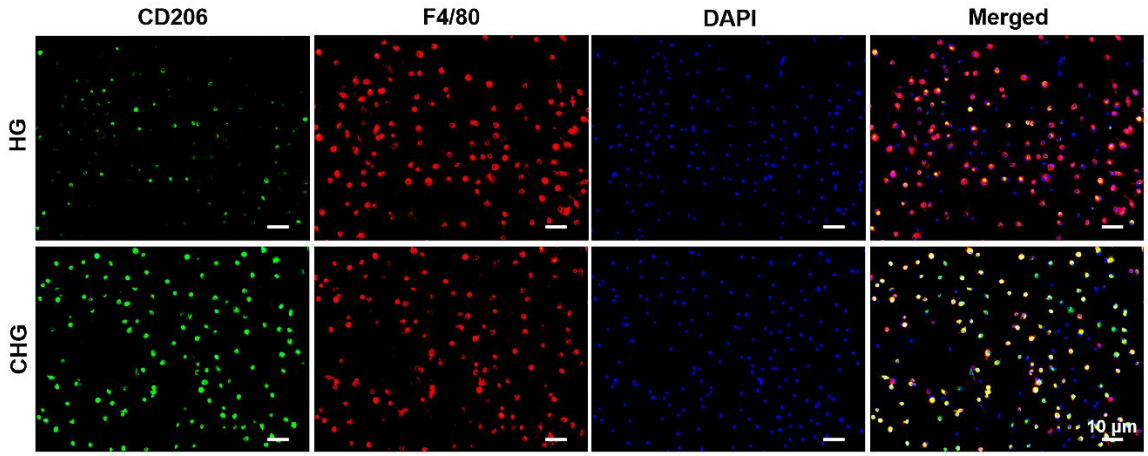

Fig. S12. CD206 and F4/80 immunofluorescence of BMMs cultured on the surface of composite hydrogels.

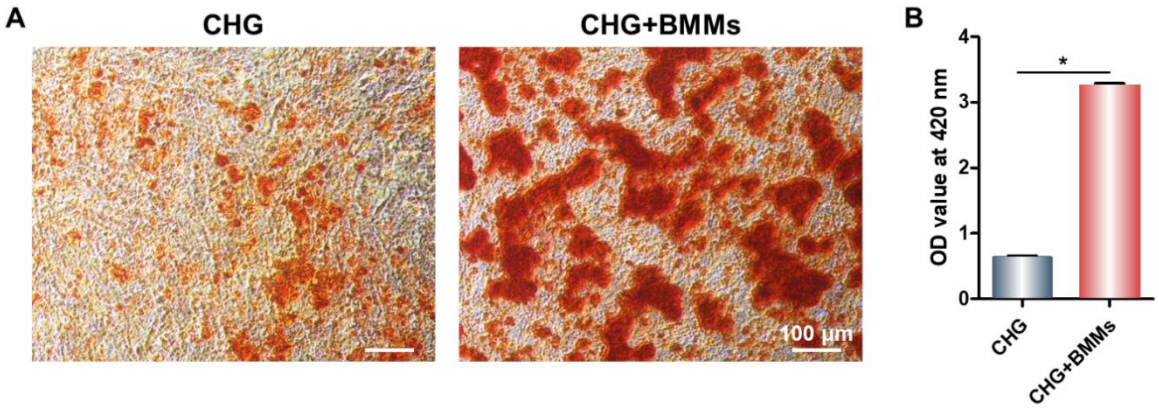

Fig. S13. Alizarin red staining (**A**) and quantitative characterization (**B**) of calcium deposition in BMSCs treated by the extract of CHG composite hydrogel and the conditioned media from BMM culture. (*$p < 0.05$)

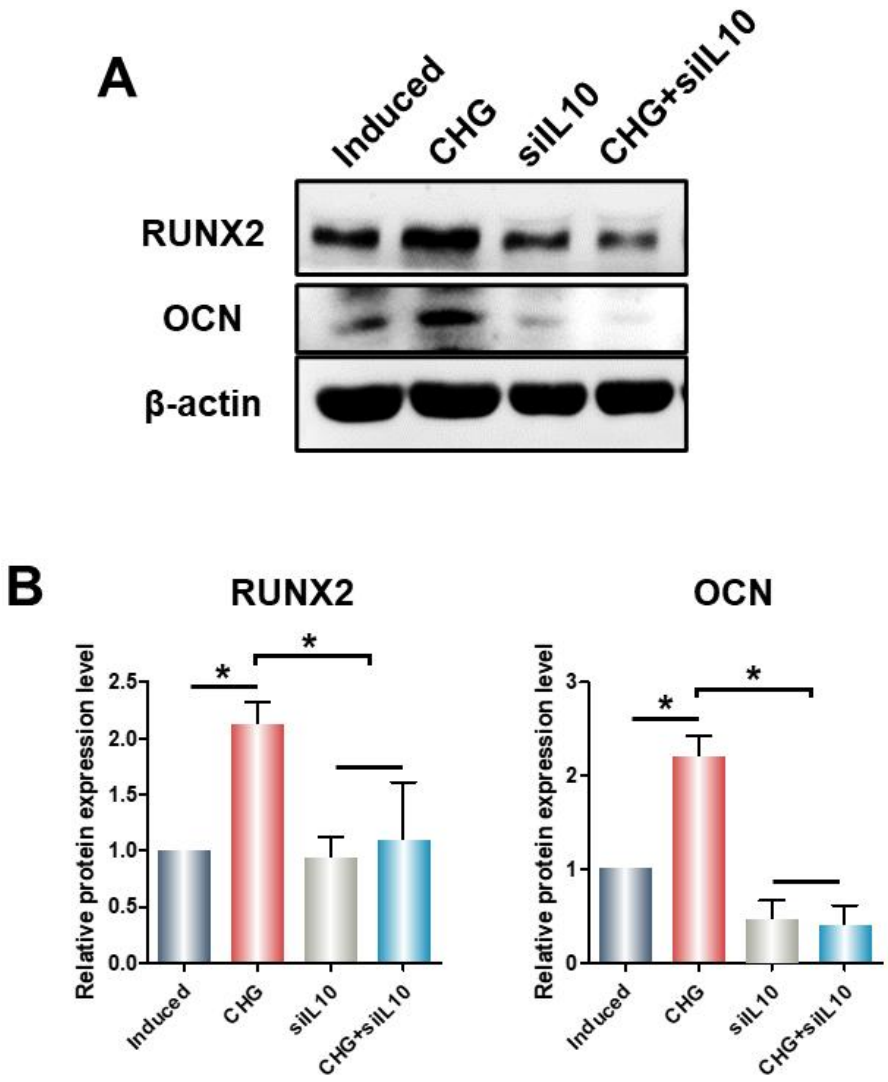

Fig. S14. Expression (**A**) and quantification (**B**) of osteogenic proteins of BMSCs cultured on the composite hydrogels. (*$p < 0.05$)

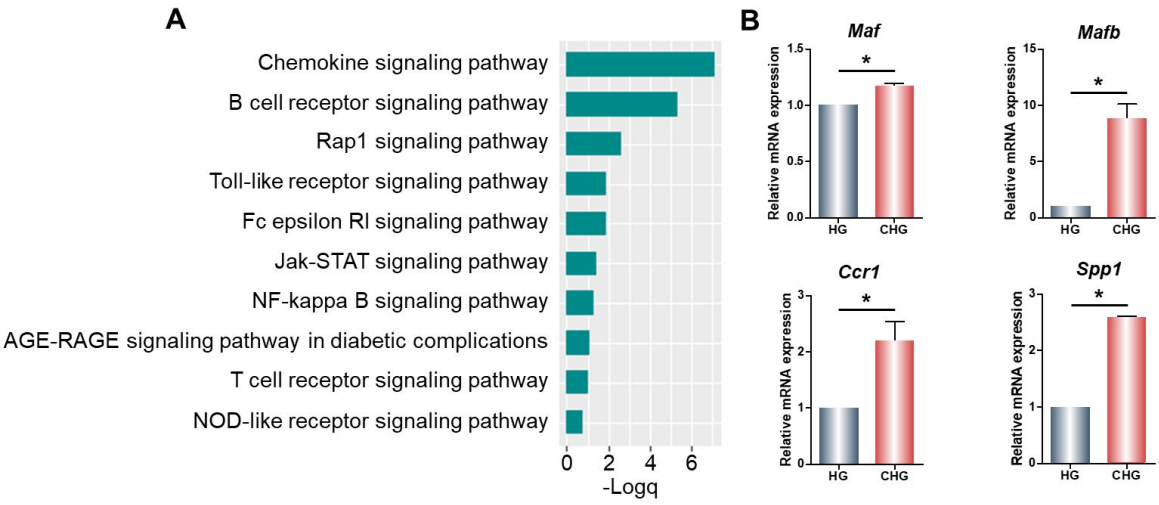

Fig. S15. KEGG signaling pathway enrichment analysis (**A**) and the expression of *Maf*, *Mafb*, *Ccr1* and *Spp1* (**B**). (*$p < 0.05$)

Table S1. PCR primer sequences.

Target	Forward primer sequence (5'–3')	Reverse primer sequence (5'–3')
Alpl	TATGTCTGGAACCGCACTGAA	CACTAGCAAGAAGAAGCCTTT
Spp1	GCGGTTCACTTTGAGGACAC	TATGAGGCGGGGATAGTCTTT
Runx2	ATCCAGCCACCTTCACTTACAC	GGGACCATTGGGAACTGATA
Col1a1	CAGGCTGGTGTGATGGGATT	CCAAGGTCTCCAGGAACACC
Bglap	AACGGTGGTGCCATAGATGC	AGGACCCTCTCTCTGCTCAC
Sirt1	GCTCGCCTTGCTGTGGACTTC	GTGACACAGAGATGGCTGGA
Sod2	GCTGGAGGCTATCAAGCGTGA	TTAGAGCAGGCGGCAATCTGT
Actin	CTCATGCCATCCTGCGTCTG	GGCAGTGGCCATCTCTTGCT